

Article

How Do Temporal and Geographical Kernels Differ in Reflecting Regional Disparities? Insights from a Case Study in China

Chunzhu Wei ¹, Xufeng Liu ¹ , Wei Chen ¹ , Lupan Zhang ¹, Ruixia Chao ^{1,*}  and Wei Wei ^{2,*}

¹ School of Geography and Planning, Southern Marine Science and Engineering Guangdong Laboratory (Zhuhai), Sun Yat-sen University, Guangzhou 510275, China; weichzh@mail.sysu.edu.cn (C.W.); liuxf65@mail2.sysu.edu.cn (X.L.); chenw297@mail2.sysu.edu.cn (W.C.); zhanglp28@mail2.sysu.edu.cn (L.Z.)

² School of Economic, Guangxi University for Nationalities, Nanning 530006, China

* Correspondence: chaorx3@mail.sysu.edu.cn (R.C.); 20070018@gxmzu.edu.cn (W.W.)

Abstract: Rapid economic growth in China has brought about a significant challenge: the widening gap in regional development. Addressing this disparity is crucial for ensuring sustainable development. However, existing studies have largely overlooked the intrinsic spatial and temporal dynamics of regional disparities on various levels. This study thus employed five advanced multiscale geographically and temporally weighted regression models—GWR, MGWR, GTWR, MGTWR, and STWR—to analyze the spatio-temporal relationships between ten key conventional socio-economic indicators and per capita GDP across different administrative levels in China from 2000 to 2019. The findings highlight a consistent increase in regional disparities, with secondary industry emerging as a dominant driver of long-term economic inequality among the indicators analyzed. While a clear inland-to-coastal gradient underscores the persistence of regional disparity determinants, areas with greater economic disparities exhibit pronounced spatio-temporal heterogeneity. Among the models, STWR outperforms others in capturing and interpreting local variations in spatio-temporal disparities, demonstrating its utility in understanding complex regional dynamics. This study provides novel insights into the spatio-temporal determinants of regional economic disparities, offering a robust analytical framework for policymakers to address region-specific variables driving inequality over time and space. These insights contribute to the development of targeted and dynamic policies for promoting balanced and sustainable regional growth.

Keywords: social disparity; spatio-temporal non-stationarity; spatial and temporal kernels; spatio-temporal patterns; geographically and temporally weighted regression models



Academic Editors: Jingzhe Wang, Yangyi Wu, Yinghui Zhang, Ivan Lizaga and Zipeng Zhang

Received: 2 December 2024

Revised: 24 December 2024

Accepted: 27 December 2024

Published: 31 December 2024

Citation: Wei, C.; Liu, X.; Chen, W.; Zhang, L.; Chao, R.; Wei, W. How Do Temporal and Geographical Kernels Differ in Reflecting Regional Disparities? Insights from a Case Study in China. *Land* **2025**, *14*, 59. <https://doi.org/10.3390/land14010059>

Copyright: © 2024 by the authors. Licensee MDPI, Basel, Switzerland. This article is an open access article distributed under the terms and conditions of the Creative Commons Attribution (CC BY) license (<https://creativecommons.org/licenses/by/4.0/>).

1. Introduction

Since the inception of the “Reform and Opening Up” policy in the late 1970s, China has experienced remarkable economic growth, with its real GDP expanding at an average annual rate of 9.8% over the past three decades [1]. However, alongside this economic development, there has been a noticeable increase in rural–urban and regional economic disparities post-2000 [2]. For instance, coastal regions exhibit a per capita GDP double that of inland areas, while Shanghai’s per capita GDP surpasses that of inland Guizhou Province by a factor of 10. Such escalating economic inequality can fuel social discontent and political instability within a nation. Moreover, considerable and swiftly escalating inequality may hamper economic growth and jeopardize the prospects of sustainable long-term development [3]. From this standpoint, addressing regional social disparity is

essential for advancement and has a beneficial impact on productivity, the economy, and the reinforcement of democracy and citizenship rights [4,5].

Regional social disparity refers to unjust disparities in opportunities, resources, and outcomes among different groups of people. These disparities can in turn contribute to the emergence of spatial disparities, characterized by uneven distributions of various socio-economic factors across varying geographical areas [2,3,6]. Importantly, these spatial disparities often exhibit non-stationarity, which refers to the phenomenon where the statistical properties of a dataset—such as its mean, variance, or relationships between variables—change over space or time rather than remaining constant. In essence, social disparity is a driving force behind the phenomenon of spatial disparity, as these two concepts are intricately interlinked and mutually reinforcing. Therefore, recognizing the spatial disparity and identifying the determinants of social disparity as a foundation for targeted policy interventions to address the unique needs and concerns of disadvantaged regions [7]. This recognition stands as the prerequisite to help implement policies that facilitate social inclusion and provide opportunities for marginalized groups to overcome structural barriers [8].

However, while the widely used global linear regression models are only able to analyze the complicated influence of socio-economic variables in social disparity [9], they neglect the spatial or temporal trends of regional disparity at some scales [10,11]. For example, ordinary least square (OLS) assumes that the regression relationship between independent variables and the explanatory variable is homogeneous in space and time, leading to the inaccuracy or failure of results in exploring disparity patterns and processes. Therefore, a series of OLS-like models, such as the expansion method [12], the distance-decay weighted regression [13], and the geographically weighted regression (GWR) model have been proposed to take spatial heterogeneity into consideration [14–16].

Among these OLS-like models, GWR was one of the widely used methods in regional economic disparity analysis [17]. GWR is widely used in rural [18] and urban [19] analyses, and the research scale ranges from large-scale administrative districts (such as the city agglomeration [20] and provincial levels [21]) to small-scale community studies in non-administrative units. In GWR, predictive variables such as the built environment (e.g., land use patterns, transportation systems, urban design variables) and socio-economic situations (e.g., income, GDP, unemployment rate, education level) are embedded within the GWR framework to demonstrate the social disparity determinants [22].

A critical component of GWR and its extensions is bandwidth optimization, which determines the spatial range (or temporal range in spatio-temporal models) over which observations influence the local regression estimates. In GWR, a single bandwidth is selected to ensure the relationships between variables are adequately smoothed while capturing local variations. However, this uniform bandwidth assumes that all relationships vary at a single spatial scale, which may oversimplify complex socio-economic phenomena [23]. To address this limitation, the multiscale GWR model (MGWR) introduces variable-specific bandwidths, enabling each predictor to adapt to distinct spatial scales. For example, while income disparity might vary significantly over a broad spatial range, unemployment effects could be more localized. MGWR's bandwidth optimization dynamically adjusts to these differences, providing a finer-grained analysis of socio-economic determinants [24–26]. Both GWR and MGWR highlight the importance of spatio-temporal kernels, which serve as weighting functions to determine the influence of observations within a specific spatial or temporal neighborhood. These kernels enable the models to capture variations in social disparity determinants across both space and time, providing a dynamic lens to analyze complex processes. By addressing the non-stationary nature of socio-economic phenomena and introducing spatio-temporal kernels, these models offer powerful tools for

exploring how social disparity determinants evolve across different spatial and temporal scales [27,28].

While it is worth noting non-stationarity in a social disparity context, it can also be the case that spatial disparity differs not only in a variety of spaces but at various times (time–non-stationarity). Thus, to improve upon the GWR and MGWR methods, geographically and temporally weighted regression (GTWR) [29,30] and multiple scales of GTWR (MGTWR) models incorporating temporal dimensions alongside spatial bandwidth optimization have been proposed to combine the effects of temporal and spatial variation in the regression model. The time variation considered in the GTWR and MGTWR model is the concept of a time interval instead of the rate of value variation over time. The stepwise strategy applied in the spatio-temporal kernel function of the GTWR and MGTWR model is to fix an optimized spatial bandwidth first, and then it fixes the optimized temporal bandwidth [31,32]. However, this time-isolated bandwidth optimization procedure does not always seem reasonable [33], as it is not able to optimize both the temporal and spatial bandwidths at the same time [34]. At present, GTWR and other improved models of GWR have been used in a large number of case studies in exploring ecological environment and urban construction [35,36], air quality and carbon cycle [37].

To further improve the spatio-temporal kernel function, the recently developed spatio-temporal weighted regression (STWR) model has been proposed by Que [38]. Different from the GTWR and MGTWR, the STWR model treats the time distance as the rate of value variation over a time interval rather than the time interval itself. This model integrates spatial and temporal bandwidth optimization into a unified framework. By weighting observations based on their proximity in both space and time, STWR excels at modeling complex processes that evolve non-uniformly across regions and periods. It is thus more suitable to consider the effects of different variation of observed points over time. In addition, STWR optimized the temporal kernel function in two or three dimensions, which is different with the one-dimension temporal kernel function (e.g., Gaussian kernel or Bi-square kernel) that defined in GTWR and MGTWR. STWR utilizes a weighted average form to calculate the spatio-temporal kernel rather than the multiplication form in GTWR and MGTWR [29,33], which may avoid potential underestimation of combined spatio-temporal effects [38].

Addressing the intricate dynamics of social disparity requires tackling complex, non-linear interactions between temporal and spatial factors. These challenges are further compounded by issues like the modifiable areal unit problem (MAUP) or “neighborhood effect” [39], which arise from variations in geographical definitions and scales. To address these complexities, this study employs advanced spatial and spatio-temporal regression models, including GWR, MGWR, GTWR, MGTWR, and STWR, which effectively account for non-stationarity across spatial and temporal dimensions—critical for analyzing socio-economic data such as GDP per capita [40].

By leveraging spatio-temporal kernels, these models capture localized variations and dynamically adapt to changes over both space and time. Their interpretability and ability to provide geographically and temporally explicit insights set them apart from machine learning techniques like random forests [41], support vector machines [42–44], or neural networks [45,46], which often function as black box approaches. Unlike machine learning models, these regression methods deliver localized coefficients, revealing spatially and temporally varying relationships that offer valuable insights into regional disparities and socio-economic patterns [47]. This interpretability makes these models particularly advantageous for policy-making and academic research, where understanding the underlying mechanisms driving disparities is as crucial as achieving predictive accuracy. Their ability

to identify nuanced, context-specific relationships supports the development of targeted interventions and evidence-based strategies to address social inequality effectively [48].

Additionally, socio-economic variables often exhibit unique spatio-temporal patterns, further complicating the analysis of regional disparities. To better understand their dynamics, this study focuses on county-level and prefecture-level cities in China as fundamental spatial units [49]. Using spatio-temporal regression models of GWR, MGWR, GTWR, MGTWR, and STWR, it aims to:

- (1) Evaluate and compare the effectiveness of GWR, MGWR, GTWR, MGTWR, and STWR in identifying and quantifying the key determinants of regional economic disparities.
- (2) Investigate how these models capture spatio-temporal heterogeneity across different administrative levels, providing deeper insights into the structural factors driving regional social disparities.

This research contributes to refining the analytical framework for studying regional disparities by integrating advanced spatio-temporal modeling techniques with a focus on scale-sensitive and context-specific socio-economic variables.

2. Study Area and Data Collection

2.1. Study Area

To thoroughly investigate the “neighborhood” effect in various geographically and temporally weighted regression models, this study examines regional disparities in China at two spatial scales: the county level (2357 counties) and the prefecture level (357 cities), as depicted in Figure 1a. The temporal dimension is segmented into four periods: 2000–2005, 2006–2010, 2011–2015, and 2016–2019. Given evidence of increasing rural–urban and regional economic disparities in China since 2000 [2], we extended the analysis to evaluate social disparities across two dimensions: (1) poverty-stricken versus non-poverty-stricken regions and (2) mega-regions and sub-national regions, represented by the southeastern and northwestern areas divided by the Hu Line. This multi-scale and multi-regional approach ensure sensitivity to the spatio-temporal dynamics of social disparity evolution.

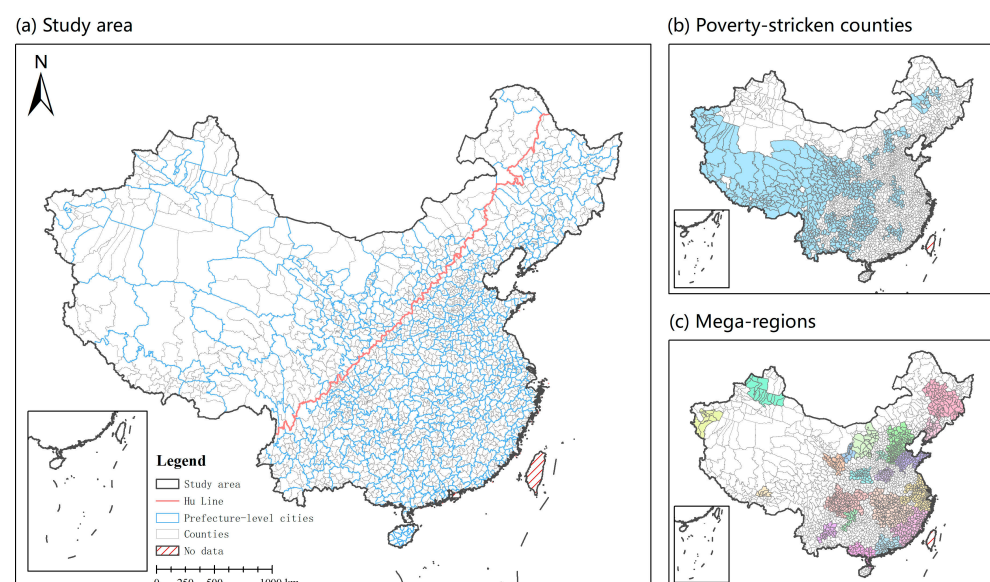


Figure 1. County-level and prefecture-level data were used to show the spatio-temporal regression. Other spatial units levels (poverty-stricken vs. non-poverty-stricken regions, mega-regions, and west/east of Hu Line regions) were used to evaluate socio-economic inequity as well as the model’s sensitivity in this study.

To address the frequent boundary changes in county-level administrative units, we employed a boundary harmonization strategy. Using the 2019 administrative boundaries of county-level units (2347 counties within 357 cities) as the authoritative reference dataset (<http://www.resdc.cn/>, accessed on 1 January 2021), we ensured consistent spatial boundaries across all time periods. This harmonization accounted for over 653 boundary changes between 2000 and 2020 [50]. When discrepancies were identified, socio-economic data such as GDP and population were adjusted to a unified base year boundary using spatial overlay techniques in GIS. For counties with boundary modifications, data were recalculated using an area-weighting method or a time series interpolation approach, ensuring comparability across years. To validate these adjustments, the recalibrated data were cross-referenced with secondary datasets to minimize discrepancies and confirm accuracy. These preprocessing methods ensured that the observed temporal trends reflected genuine socio-economic changes rather than artifacts introduced by administrative boundary modifications.

2.2. Variables

How to objectively measure socio-economic inequity is a key issue in a regional disparity study. Gross domestic product (GDP) per capita is an indicator that is widely used in socio-economic research [17,27], and the growth rate of real GDP per capita has shown a significant influence on regional development. This indicator is more generic across regions compared with other indicators such as GDP, minimum income, etc. Thus, this study adopted GDP per capita as the dependent variable to depict regional disparities in China.

We selected the independent variables based on a comprehensive literature review and data availability [42,43]. To clarify the rationale behind our selection, we have provided the following explanations: (1) Practitioner number (PN) reflects the active labor force, a key driver of economic productivity and GDP growth [51]. (2) Primary industry (PI) includes agriculture, forestry, and fishing, representing the backbone of rural economies and regional economic transitions [52]. (3) Secondary industry (SI) captures industrial production and urbanization, a major GDP growth driver in emerging economies [53]. (4) Public financial revenue (PFR) indicates government income for funding infrastructure and services, linked to economic growth and decentralization [54]. (5) Public financial expenditure (PFE) reflects government spending on public goods associated with growth and social welfare [55]. (6) Deposit balance (DB) represents household savings and financial stability, influencing inequality and consumption [56]. (7) Loan balance (LB) highlights access to credit and investment capacity, crucial for economic development [57]. (8) Total power of agricultural machinery (TP) indicates mechanization, boosting agricultural productivity and rural economic transformation [58]. (9) Student number (SN) reflects educational access, fostering human capital and long-term growth (Becker, 1964). (10) Hospital bed number (HBN) measures healthcare infrastructure, linked to workforce productivity and social development [59]. (11) Grain yield (GY) indicates agricultural productivity, essential for food security and rural stability [60].

These variables were chosen to explore GDP determinants across spatial and temporal contexts. PN, PI, and GY highlight disparities in employment and agriculture-dependent regions. SI addresses industrialization-driven disparities. PFR and PFE reflect government capacity and investment. DB and LB capture financial inclusion and savings patterns, while TP, SN, and HBN emphasize rural development, education, and healthcare. A detailed description of these variables is provided in Table 1.

Table 1. Summary of the variables used.

Variable Type	Variable Name	Code	Description
Dependent variables	Gross domestic product per capita	GPC	Gross domestic product divided by population
	Practitioner number	PN	Number of registered practitioners
	Primary industry	PI	GDP of primary industry
	Secondary industry	SI	GDP of secondary industry
	Public financial revenue	PFR	Total public financial revenue of the government
	Public financial expenditure	PFE	Total public financial expenditure of the government
Independent variables	Deposit balance	DB	Total saving deposits of urban and rural residents
	Loan balance	LB	Balance of various loans of financial institutions at the end of the year
	Total power of agricultural machinery	TP	The sum of the rated power of all agricultural machinery power
	Student number	SN	Number of students in primary and secondary schools
	Hospital bed number	HBN	Number of beds in medical and health institutions
	Grain yield	GY	Total grain yield of each county

The variance inflation factors (VIFs) for 10 of the explanatory variables were all below the acceptable threshold of 10 (ranging from 2.38 to 9.29) across four years of analysis. For public financial revenue (PFR), the VIF exceeded 10 in earlier years but fell below this threshold in 2014 and 2019. PFR was retained in the analysis because it serves as a critical proxy for regional government capacity to invest in development initiatives. It reflects government income from taxes and other sources that fund public services and infrastructure development. Given its historical alignment with economic expansion and fiscal decentralization, PFR provides valuable insights into regional disparities. To ensure comprehensive analysis, we included all 11 variables, as their collective impact is integral to understanding the socio-economic dynamics in this study. This approach balances statistical robustness with the inclusion of theoretically and empirically significant variables, as detailed in the methodology section. The details of the VIFs are shown in Tables S3–S6 in the Supplementary Materials. All the socio-economic statistic data from 2000 to 2019 were collected from the China County Statistical Yearbook (CCSY), published by the National Bureau of Statistics of China. All of these data are publicly available.

3. Methodology

As shown in Figure 2, the research methodology in this study involved two major steps: (1) OLS, GWR, MGWR, GTWR, MGTWR, and STWR model regression; the relationship between the dependent and independent variables was established using the six regression models; and (2) comparison between the results of the OLS, GWR, MGWR, GTWR, MGTWR, and STWR models. A calibration procedure was implemented to optimize the bandwidth of the regression models according to R^2 and the Akaike information criterion (AIC), and then the spatio-temporal heterogeneity of different variables was explored across two different spatial domains.

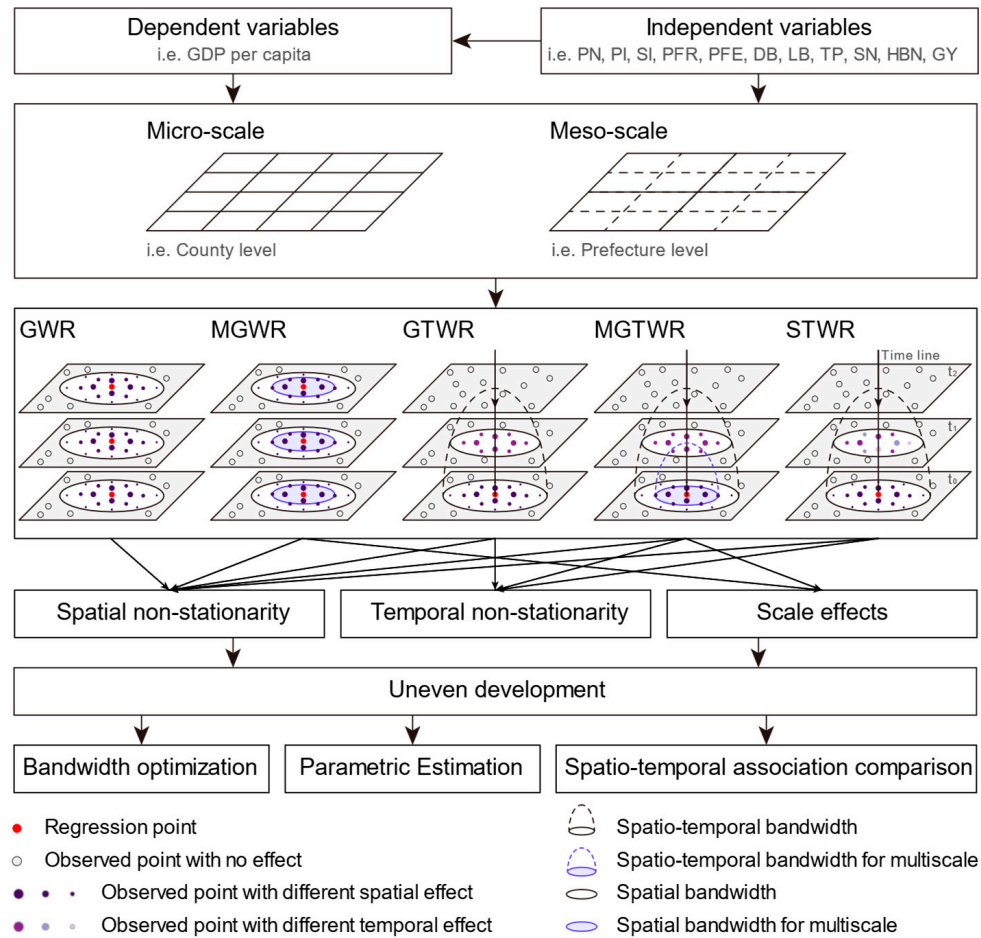


Figure 2. Workflow of the methodology.

3.1. GWR Model

Traditionally, the relationship between the dependent and independent socio-economic variables has been built using ordinary least squares (OLS) regression, i.e.,

$$y_i = \beta_0 + \sum_{k=1}^m \beta_k x_{ik} + \varepsilon \tag{1}$$

where β_0 represents the intercept value, and β_k denotes the k th coefficient, and k is assumed to be 11 in this study. x_{ik} represents the k th independent variable, and y_i represents the dependent variable.

Based on the OLS model, the GWR methodology was proposed, which used local regression framework to explain spatial non-stationarity by estimating various parameters locally in space [14]. The parameters were estimated locally, using distance-weighted subsampling at neighboring locations, which can be expressed as:

$$y_i = \beta_0(u_i, v_i) + \sum_{k=1}^m \beta_k(u_i, v_i) x_{ik} + \varepsilon_i \tag{2}$$

where y_i is a response variable of point i at location i with the coordinate (u_i, v_i) , and x_{ik} represents the k th in m predictive variables of point i . $\beta_0(u_i, v_i)$ is the intercept value, $\beta_k(u_i, v_i)$ denotes the estimated parameter for the k th predictor variables, and ε_i is the error term of point i . $\beta_k(u_i, v_i)$ in the GWR model is estimated using the predictive variables of point i 's neighbors in the scope defined by the space distance to the point i and can be expressed by Equation (3):

$$\beta_k(u_i, v_i) = [X^T W(u_i, v_i) X]^{-1} X^T W(u_i, v_i) y \quad (3)$$

where X is the independent variable matrix, X^T is the transpose of X , y is the independent variable, and $W(u_i, v_i)$ denotes an $n \times n$ diagonal geographic weighting matrix for point i , which is formed through a kernel function, such as Gaussian and bi-square. Here $\beta_k(u_i, v_i)$ denotes the impact of x_{ik} on y_i (GDP per capita in this case), and higher $\beta_k(u_i, v_i)$ signifies larger impact on regional economic disparity.

3.2. MGWR Model

MGWR is an extension of GWR. While GWR assumes consistent local relationships across models at the same spatial scale [24], MGWR allows the conditional relationships between the response variable and the different predictor variables to vary at different spatial scales. This adaptability is facilitated by aligning each explanatory variable's neighborhood with its own spatial extent, a principle that underpins MGWR's enhanced coefficient estimation within local regression models. This innovation is reflected in the bandwidths, which indicate the range over which data is borrowed and can vary by parameter surface. The expression of MGWR Equation (4) is refined from Equation (2).

$$y_i = \beta_0(u_i, v_i) + \sum_{k=1}^m \beta_{bwk}(u_i, v_i) x_{ik} + \varepsilon_i \quad (4)$$

Assuming that there are n observations, for observation $i \in \{1, 2, \dots, n\}$ at location (u_i, v_i) , bw_k in β_{bwk} indicates the bandwidth used for the calibration of the j th conditional relationship.

3.3. GTWR Model

To further reveal the influence of spatial-temporal heterogeneity of independent variables, the GTWR model is used to explore regional differences and periodic laws of influencing effects [33,61]. The base formula of the GTWR model is shown as follows:

$$y_i = \beta_0(u_i, v_i, t_i) + \sum_{k=1}^m \beta_k(u_i, v_i, t_i) x_{ik} + \varepsilon_i \quad (5)$$

where y_i is the response variable at point i with spatial and temporal coordinates (u_i, v_i, t_i) . In GTWR, $\beta_k(u_i, v_i, t_i)$ is optimized using the predictive variables of point i 's neighbors in the scope defined by the space-time distance to the point i , and it can be obtained from Equation (6), where $W(u_i, v_i, t_i)$ is a diagonal spatio-temporal weighting matrix specific to location i :

$$\beta_k(u_i, v_i, t_i) = [X^T W(u_i, v_i, t_i) X]^{-1} X^T W(u_i, v_i, t_i) y \quad (6)$$

The elements in the spatio-temporal weighting matrix can be represented as:

$$W(u_i, v_i, t_i) = \begin{cases} W_{ij}^S \times W_{ij}^T, & 0 \leq \Delta t < b^{S\tau} \\ 0, & \text{otherwise} \end{cases} \quad (7)$$

$$W_{ij}^T = \exp\left(-\frac{d_{ij}^T}{h_T}\right), \quad W_{ij}^S = \exp\left(-\frac{d_{ij}^S}{h_S}\right)$$

$$d_{ij}^T = \sqrt{(t_i - t_j)^2} \quad (t_i > t_j) \quad d_{ij}^S = \sqrt{(u_i - u_j)^2 + (v_i - v_j)^2}$$

where W_{ij}^T and W_{ij}^S are the time-weighted and space-weighted elements between observations i and j , respectively. h_T and h_S are the spatial-temporal bandwidth. d_{ij}^S is defined as the spatial distance between observations i and j ; v is the bandwidth in time. τ is used for adjusting the inconsistency of the time distance and space distance, and therefore $b^{S\tau}$ is

the spatial bandwidth b^S at a certain time stage τ , and b^T denotes the temporal bandwidth. The remaining steps of GTWR are similar to those in GWR.

3.4. The MGTWR Model

The calibration of the MGTWR model is based on a back-fitting algorithm, and the MGTWR model is regarded as a generalized additive form [25]:

$$y_i = \beta_0(u_i, v_i, t_i) + \sum_{k=1}^m \beta_{bwk}(u_i, v_i, t_i)x_{ik} + \varepsilon_i = \sum_{k=1}^m f_{ik} + \varepsilon_i \quad (8)$$

The MGTWR model regression coefficients bwk for the k th covariate are calibrated using the specific bandwidth bwk . The back-fitting algorithm first initializes the additive term vector $f_k = [f_{1,k}, f_{2,k}, \dots, f_{n,k}]$ using the GTWR model. The residual term $\hat{\varepsilon}$ at this stage can be obtained from $\hat{\varepsilon} = y - \sum_{k=1}^m f_k$. The first covariate generates the optimal bandwidth $bw1$ and updates the first additive term vector f_k as well as $\hat{\varepsilon}$. Then this process continues on to the next covariate until all optimal bandwidths bwk are updated.

3.5. STWR Model

The spatio-temporal weighted regression model (STWR) is a space–time regression model similar to GTWR to explore local spatio-temporal non-stationarity. The most notable improvement of STWR compared with GTWR is that it is designed to have a weighted average form in the spatio-temporal weighting matrix [38]. The distances are calculated as:

$$W_{ij}^{ST} = (1 - \alpha)W_{ij}^S + \alpha W_{ij}^T \quad (9)$$

where $\alpha \in [0, 1]$ is an adjustable factor to scale the space and time effect. This improves on the potential weight underestimation and accelerates the calculation through kernel functions. W_{ij}^S is the same as in the GTWR model and W_{ij}^T is not the time interval, but the rate of value variation between an observed point and a regression point through a time interval, shown as follows:

$$W_{ij}^T = \begin{cases} \left[\frac{2}{1 + \exp(-d_{ij}^T/b^T)} - 1 \right], & 0 < \Delta t < b^T \\ 0, & \text{otherwise} \end{cases} \quad (10)$$

$$d_{ij}^T = \frac{|(y_i - y_j)/y_j|}{t_i - t_j} \quad (11)$$

where Δt is the time interval $t_i - t_j$ between point i and point j , and b^T is the temporal bandwidth selected from time intervals. d_{ij}^T represents spatial distance and temporal distance between point i and point j , respectively, t_i is the timestamp of point i , and t_j is the timestamp of point j ($t_j < t_i$); y_i and y_j are dependent variables. Thus, d_{ij}^T is actually the rate of value variation from time t_j to t_i , rather than the time interval, as in GTWR.

3.6. Model Evaluation

The above algorithms were implemented in the package of GWmodel and STWR v1.0 model in Python [38,62]. To avoid randomness within different regression models as well as to ensure the stability of the model results, we repeated the simulation experiment 200 times for each model for the purposes of selecting the minimum Akaike information criterion (AICc) to define the bandwidth of the model. Then several corresponding indicators, namely the mean absolute error (MAE), the root mean square error (RMSE), the coefficient of determination (R^2), and the adjusted R^2 ($Radj^2$), to quantitatively evaluate the similarity between the observations and the estimated values of the resulting response variable.

High R^2 and low RMSE, MAE, and AICc indicate a good fit between the model and the observation.

4. Results

4.1. Statistical Evaluation of the Six Regression Models

Before using the regression models, the spatial–temporal non-stationarity of explanatory variables was evaluated using the interquartile range (IQR). The IQR measures the spread of the middle half of the data, and a larger IQR value indicates a larger data variability. Comparison of the IQR of the regression coefficients from the GWR, MGWR, GTWR, MGTWR, and STWR models with twice the standard error (SE) from the OLS model is shown in Table 2. The extra local variation in the rightmost column indicated that all 11 explanatory variables exhibit spatio-temporal non-stationarities.

Table 2. The comparison of interquartile range of the regression coefficients from the GWR, MGWR, GTWR, MGTWR, and STWR models.

Variable	IQR (GWR)	IQR (MGWR)	IQR (GTWR)	IQR (MGTWR)	IQR (STWR)	$2 \times SE$ (OLS)	Extra-Local Variation
PN	0.19	0.19	0.19	0.11	0.20	0.14	Yes
PI	0.14	0.20	0.16	0.09	0.17	−0.13	Yes
SI	0.69	0.05	0.86	0.57	0.80	0.10	Yes
PFR	0.69	0.04	0.74	0.65	0.51	1.48	Yes
PFE	0.4	0.07	0.43	0.27	0.34	0.33	Yes
DB	0.63	0.04	0.78	0.47	0.75	−0.08	Yes
LB	0.70	0.03	0.76	0.40	0.67	0.19	Yes
TP	0.12	0.12	0.15	0.09	0.16	−0.04	Yes
SN	0.25	0.13	0.30	0.17	0.28	0.01	Yes
HBN	0.15	0.16	0.13	0.12	0.10	−0.34	Yes
GY	0.18	0.10	0.22	0.13	0.14	−0.09	Yes

Table 3 presents a comparative analysis of the average fitted results obtained from five regression models at two levels. At the county level, the statistical results of the STWR model exhibited the highest R^2 values of 0.97 along with the lowest AICc value for the fitting results at the county level, and relatively high R^2 values of 0.95 with reasonable RMSE and MAE values at the prefecture-level. However, at the prefecture-level, the GTWR model outperformed another four models with the highest R^2 and R_{adj}^2 , as well as the lowest RMSE and MAE values.

Comparing the performances of STWR and MGTWR models with GTWR revealed that, based on R^2 , R_{adj}^2 , and AICc values, they exhibited similar capabilities, without one model clearly surpassing the others. However, when assessing the RMSE and MAE values, STWR and MGTWR did not outperform GTWR. Therefore, these results indicate that the STWR, GTWR, and MGTWR models offer advantages over OLS, GWR, and MGWR in the fitting process. Still, they do not distinctly outperform each other based on different validation methods.

Table 3. Statistical evaluation of the OLS, GWR, MGWR, GTWR, MGTWR, and STWR models.

Level	Model	R ²	R _{adj} ²	AICc	RMSE	MAE
County	OLS	0.68	0.68	−7668.20	0.03	0.02
	GWR	0.93	0.90	−9631.55	0.02	0.01
	MGWR	0.93	0.90	−9278.35	0.02	0.01
	GTWR	0.97	0.95	−49,311.54	0.02	0.01
	MGTWR	0.94	0.92	−49,579.53	0.02	0.01
	STWR	0.97	0.95	−11,380.14	0.02	0.01
Prefecture	OLS	0.70	0.69	−808.76	0.13	0.09
	GWR	0.86	0.81	−898.94	0.05	0.03
	MGWR	0.86	0.81	−853.78	0.05	0.03
	GTWR	0.96	0.94	−5625.34	0.12	0.08
	MGTWR	0.95	0.92	−4317.74	0.12	0.08
	STWR	0.95	0.92	−1228.29	0.20	0.14

4.2. Spatial Dynamics of the Beta Parameter for the 11 Variables in Response to GDP per Capita

During the study period, the mean nominal GDP per capita exhibited a consistent increasing trend across both county- and prefecture-level regions (Figure 3b), with the most significant growth observed between 2005 and 2015. After adjusting for the GDP deflator coefficients provided by the National Bureau of Statistics (2000: 0.35%; 2005: 1.78%; 2010: 3.18%; 2015: 1.44%; 2019: 2.90%), the trend of real GDP per capita mirrored that of nominal GDP per capita (Figure 3b). However, regional disparities in GDP per capita widened significantly after 2005.

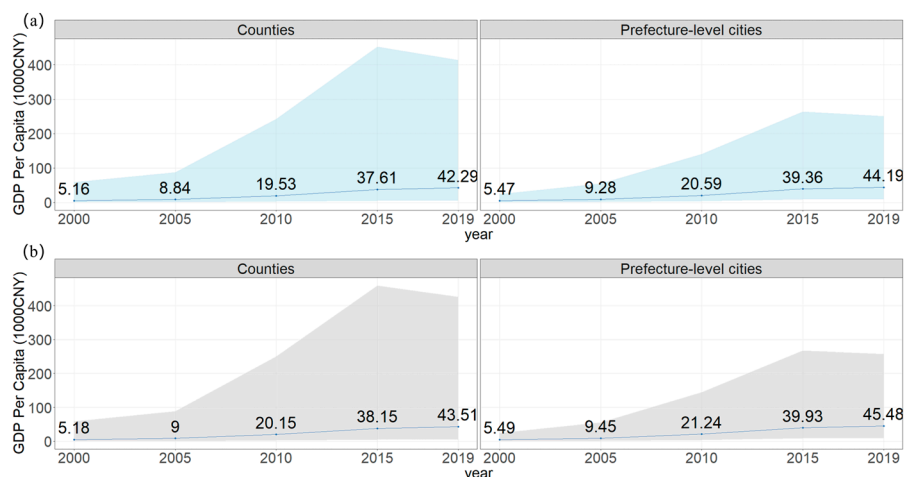


Figure 3. The regional differences based on real GDP per capita (a) and nominal GDP per capita (b) from 2000 to 2019. The blue dots represent the regional mean value, and the shaded area represents the variance.

Specifically, regional differences in GDP per capita increased modestly during the first five years but grew rapidly over the subsequent 15 years. The growth rates of mean GDP per capita were 740.1% and 728.2% at the county and prefecture levels, respectively. Although the regional per capita differences at the prefecture level were initially less than half of those at the county level during the first decade, these disparities continued to expand after 2015. In contrast, per capita differences at the county level began to narrow during this period.

Among the 11 independent variables, secondary industry (SI) has always had the most positive influences and made the biggest contribution to the GDP per capita over the past 20 years. While the relationships between GDP per capita and the other variables vary dramatically—for example, in 2000, SI, PN and SN were three of the most important variables related to the GDP per capita at the prefecture level, but the variables’ combination changed to SI, PN, and DB in 2010 and SI, PFR, and HBN in 2019. Therefore, we only selected the SI, PN, and HBN variables in 2019 as an example to further demonstrate the spatial pattern variances of their intercept coefficients in response to GDP per capita.

As shown in the spatio-temporal regression results in Figures 4 and 5, based on five models, SI maintained a positive and significant influence on GDP per capita using different models across county-level and prefecture-level regions, and the highest value was observed in the northwestern regions of China. Following SI, PFE also showed a gradient spatial pattern from the southeastern parts to the northwestern parts of China. Unlike SI and PFE, the spatial pattern of HBN is more diverse across the study regions.

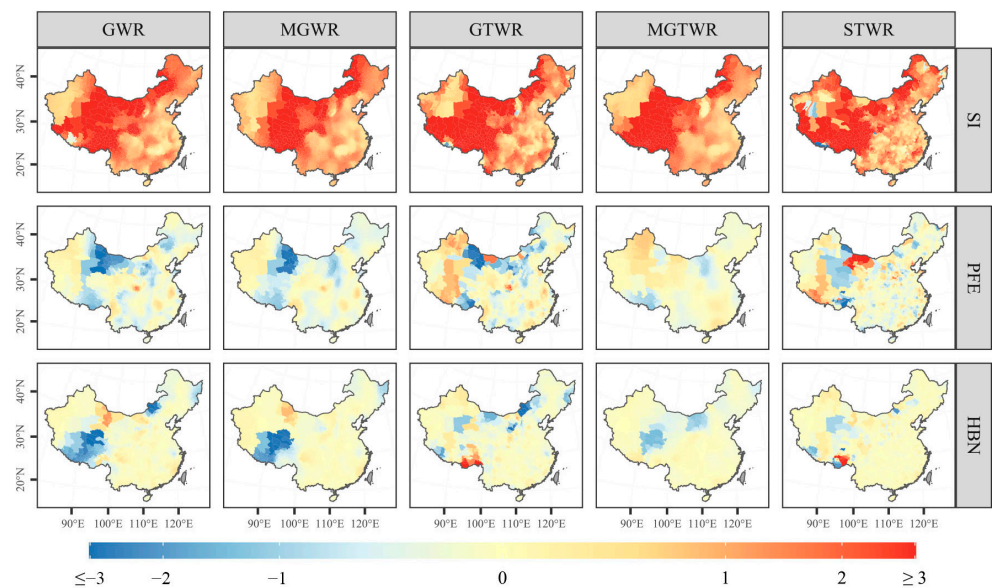


Figure 4. The spatial patterns of the β_k parameter for the predictive variables in 2019 at the county level.

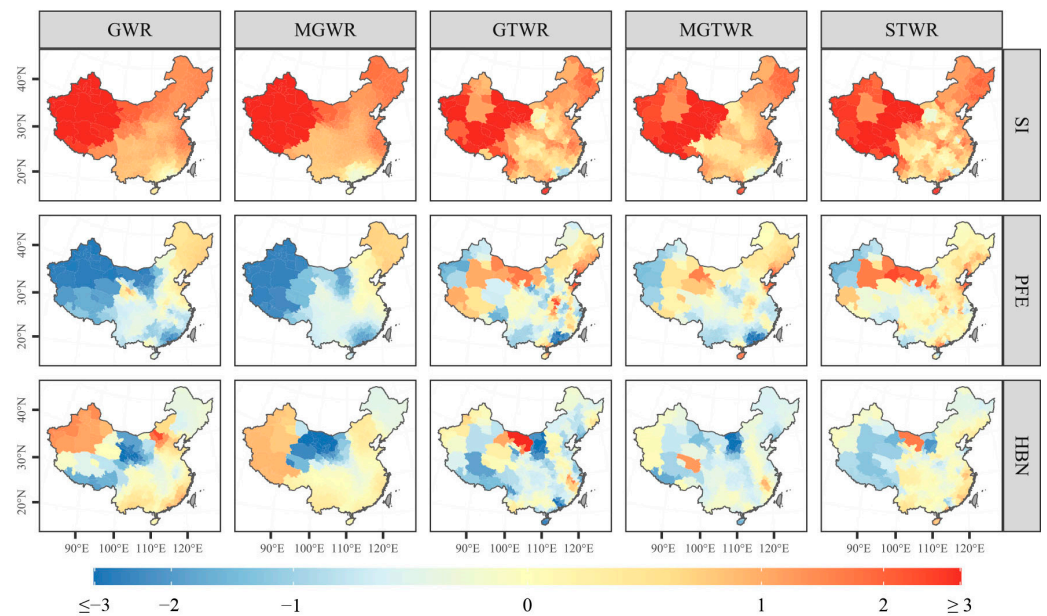


Figure 5. The spatial patterns of the β_k parameter for the predictive variables in 2019 at the prefecture level.

In term of the models' performance, the spatial pattern of intercept coefficients based on the STWR model was more consistent with that based on the GTWR model and MGTWR model. Comparatively, the spatial patterns of intercept coefficients based on GWR and MGWR were less fragmented than those of STWR, GTWR, and MGTWR. In addition, when compared with the results based on county-level and city-level regions, the variances in PFE and HBN at the prefecture level are less significant than those at the county level in the southeastern part of China as well as the western part of China, and most of the intercept coefficients changed from the negative value to the positive values across these regions. Generally, the spatial patterns of intercept coefficients based on GTWR, MGTWR, and STWR are more sensitive to the variables, as well as the spatial units.

4.3. Spatial Heterogeneity of Regional Disparity Influencing Variables

Figure 6 provides a deeper insight into the spatio-temporal patterns of SI intercept coefficients over five different years, using various regression models. Notably, when it comes to the SI variable, GTWR sometimes falls short in detecting changes in parameter fitting as effectively as GWR. For instance, in 2010, significant variations were observed in SI parameters within the region at the intersection of Qinghai and Tibet Provinces. While GTWR employs an adjustment factor τ to balance the influence of time and space, it tends to over-emphasize the temporal effects in most Chinese counties while neglecting spatial fitting within local neighborhoods.

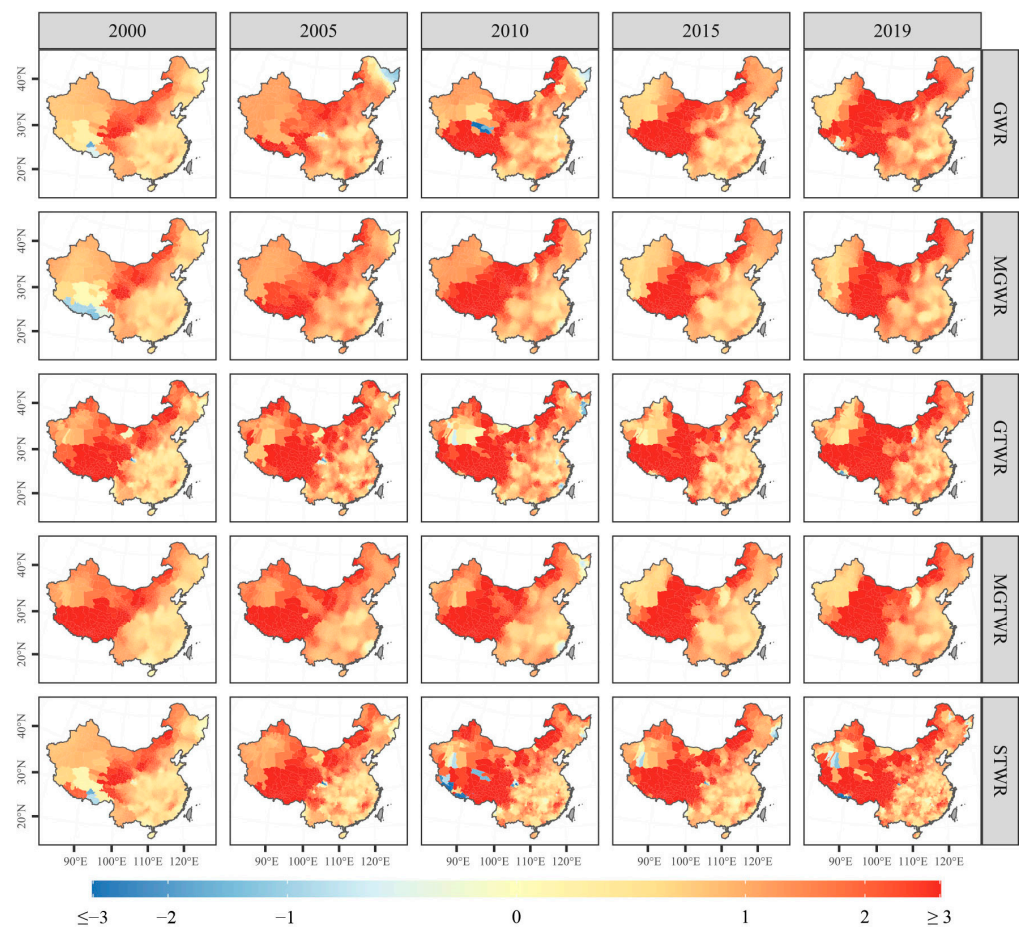


Figure 6. Spatio-temporal pattern of the the β_k parameter for SI for different models at the county level.

Furthermore, regarding the spatio-temporal patterns of SI intercept coefficients, the variations within the MGWR and MGTWR models are relatively insignificant. This suggests

that the utilization of time intervals as temporal weights through the adjustment factor c in MGTWR is not as impactful as the rate of variation in SI attribute values. In contrast, STWR excels in capturing the combined effects of a non-stationary spatio-temporal process involving the observed SI variable, effectively capturing local SI influences on GPC in both space and time. This results in more pronounced spatio-temporal variations when compared to MGWR and MGTWR.

5. Discussion

5.1. The Optimization of Bandwidth Selection in Different Models

The optimization of the spatio-temporal kernel function in STWR is distinguished by the introduction of a scale parameter, which adjusts the relative contributions of spatial and temporal kernels to the regression points. This parameter effectively quantifies the relative strength of spatial and temporal influences, enabling a more nuanced analysis of spatio-temporal interactions. However, the advantages of this optimization may not be immediately evident when temporal variations are minimal [34]. For example, as illustrated in Table 4, during the initial period (2000–2005), the R^2 values across the five models are similar. This is because models such as STWR, GTWR, and MGTWR lack prior temporal observations to leverage, and any observed R^2 differences are likely due to variations in their spatial bandwidth search ranges.

As the time intervals extend (e.g., from 5 years to 20 years), significant differences begin to surface. Models like GWR and MGWR demonstrate a consistent decline in R^2 values across the time stages, indicating reduced model fit over longer periods. In contrast, STWR maintains consistently high R^2 values, reflecting its robustness in capturing spatio-temporal dynamics. Although MGTWR occasionally achieves higher R^2 values than STWR, its performance comes with a trade-off in model complexity, as evidenced by substantially higher AICc values. AICc penalizes models with excessive complexity, balancing model fit against overfitting risks.

Table 4. Bandwidth comparison of the five models based on the bi-square kernel.

Level	Year	Model	R^2	AICc
County	1999	MGWR	0.95	−10,622.3
		MGTWR	0.95	−10,347.9
		GWR	0.95	−11,088.7
		GTWR	0.95	−11,078.8
		STWR	0.96	−11,032.9
	2004	MGWR	0.94	−9208.77
		MGTWR	0.95	−20,219.7
		GWR	0.94	−9560.87
		GTWR	0.95	−20,724.8
		STWR	0.96	−10,285.9
	2009	MGWR	0.94	−9286.07
		MGTWR	0.95	−29,307.6
		GWR	0.93	−9572.26
		GTWR	0.95	−30,821.3
		STWR	0.96	−10,114.4

Table 4. Cont.

Level	Year	Model	R ²	AICc
County	2014	MGWR	0.92	−8829.88
		MGTWR	0.96	−35,262.5
		GWR	0.92	−9044.22
		GTWR	0.95	−40,490.7
		STWR	0.93	−9904.19
	2019	MGWR	0.93	−8444.73
		MGTWR	0.94	−49,579.5
		GWR	0.93	−8891.7
		GTWR	0.97	−49,311.5
		STWR	0.97	−11,380.1
Prefecture	1999	MGWR	0.89	−782.94
		MGTWR	0.92	−738.84
		GWR	0.92	−872.11
		GTWR	0.92	−873.75
		STWR	0.93	−871.55
	2004	MGWR	0.85	−968.72
		MGTWR	0.93	−1722.67
		GWR	0.83	−956.22
		GTWR	0.93	−2055.85
		STWR	0.92	−1131.59
	2009	MGWR	0.85	−760.3
		MGTWR	0.95	−2556.34
		GWR	0.89	−873.24
		GTWR	0.95	−3221.36
		STWR	0.98	−1286.9
2014	MGWR	0.82	−915.43	
	MGTWR	0.95	−3388.8	
	GWR	0.79	−899.6	
	GTWR	0.95	−4317.06	
	STWR	0.97	−1238.52	
2019	MGWR	0.88	−841.5	
	MGTWR	0.97	−5434.55	
	GWR	0.89	−893.54	
	GTWR	0.96	−5625.34	
	STWR	0.95	−1228.29	

Furthermore, our comprehensive examination of parameter bandwidths across the five regression models highlights an important distinction: while STWR may not offer the same degree of flexibility in adjusting parameter bandwidths as the MGWR and MGTWR models [63,64], it consistently exhibited smaller bandwidths for all 11 parameters compared to their counterparts in other models. For instance, as demonstrated in Table 5, regardless of whether we considered county or city scales, the bandwidths for all parameters in STWR were 15 and 9, respectively. These values were significantly smaller than those observed

in other models. These smaller bandwidths indicate that STWR optimizes fewer initial neighbors, focusing on a more confined local area for spatio-temporal analysis.

Table 5. Bandwidth of the five models based on the bi-square kernel.

Level	Model	PN	PI	SI	PFR	PFE	DB	LB	TP	SN	HBN	GY
County	MGWR	43	43	43	43	43	43	43	43	43	43	47
	MGTWR	54	54	54	54	54	54	54	54	54	54	54
		GWR: 81			GTWR: 67		STWR: 15					
Prefecture	MGWR	43	43	46	46	43	43	43	44	44	44	51
	MGTWR	22	20	17	24	14	19	21	29	17	20	23
		GWR: 83			GTWR: 70.1		STWR: 9					

This reduced bandwidth demonstrates STWR’s capability to effectively address spatio-temporal non-stationarity within localized contexts. By focusing on smaller neighborhoods, STWR enhances the robustness of its regression outcomes, allowing it to capture finer-grained variations in the spatio-temporal dynamics of the data. This localized focus not only improves the interpretability of the results but also highlights STWR’s ability to maintain stability and accuracy in regions with complex or heterogeneous spatio-temporal patterns. Moreover, while MGTWR may occasionally achieve a higher fit, the findings emphasize that STWR offers a more optimal balance between goodness of fit and model parsimony. By avoiding excessive model complexity, STWR ensures greater reliability and interpretability across varying temporal scales. This balance underscores STWR’s practicality and effectiveness as a tool for spatio-temporal analysis, particularly in applications where achieving both precision and simplicity is essential.

5.2. The Kernel Function of Different Spatio-Temporal Regression Model

It is worth noting that the STWR model optimizes the weight matrix for spatial and temporal intervals rather than the spatial kernel function. Traditional kernel density estimation methods, such as the bi-square kernel and Gaussian kernel, incorporate a distance decay function that assigns more weight to observations closer to a regression point and less weight to those farther away [16,65]. Therefore, we also compared the performance of the bi-square kernel and Gaussian kernel in specifying spatial weighting. Since the Gaussian model has not been fully implemented in the STWR model, we only compared its results in four other models. As shown in Tables 6 and S1, all the models achieved higher R-squared values but also higher AIC information criteria when using the Gaussian kernel [25,39]. The Gaussian kernel demonstrates higher uncertainty than the bi-square kernel.

Furthermore, we compared the bandwidth differences between the Gaussian and bi-square kernels (Table 6 vs. Table S2) and found that the bandwidths for all 11 parameters were more diverse with the Gaussian kernel. This may be because the bi-square weight assigns a weight of zero to observations outside the bandwidth, effectively eliminating their influence on the local regression estimate. As a result, the bi-square kernel is less sensitive to detecting variations in the magnitudes of observation values. However, it excels in capturing local spatial heterogeneity effects from observations to the regression point.

Table 6. The comparison of bi-square and Gaussian-based models.

Level	Model	Gaussian		Bi-Square	
		R ²	AICc	R ²	AICc
County	OLS	0.68	−7668.20	0.68	−7668.20
	GWR	0.90	−9131.82	0.93	−9631.55
	MGWR	0.82	−8659.29	0.93	−9278.35
	GTWR	0.73	−39,537.20	0.97	−49,311.54
	MGTWR	0.88	−45,273.30	0.94	−49,579.53
	STWR	/	/	0.97	−11,380.14
Prefecture	OLS	0.70	−808.76	0.70	−808.76
	GWR	0.83	−868.43	0.86	−898.94
	MGWR	0.75	−836.39	0.86	−853.78
	GTWR	0.78	−4420.36	0.96	−5625.34
	MGTWR	0.88	−4990.48	0.95	−4317.74
	STWR	/	/	0.95	−1228.29

5.3. The First Law of Geography and the MAUP Issue in the Spatio-Temporal Regressions

Tobler’s First Law Of Geography [66], which states that “everything is related to everything else, but near things are more related than distant things,” serves as the foundational principle for spatial–temporal geographic weighted regression. This principle underpins the analysis of spatial heterogeneity and temporal dynamics, enabling a more nuanced understanding of geographic patterns. The findings depicted in Figure 7 further affirm this fundamental principle by illustrating the coefficient consistency of parameters across various spatial–temporal geographic weighted regression models. Consistent with Zhang [67] and Li et al. [68], this homogeneity arises from uniform socio-economic conditions, smaller GDP per capita differences, and limited industrial diversification. Similar trends are discussed by Song et al. [69] and Chen [70], who note minimal disparities in western China due to slower economic integration and less diverse economic structures.

Conversely, regions with greater GDP per capita disparities, such as the Mega-region and areas east of the Hu Line, show lower spatial consistency due to significant economic heterogeneity and rapid industrialization. Kanbur and Zhang [71] and Gao et al. [72] highlight how diversification and income disparities in these regions create fragmented spatial patterns. Advanced models like GTWR, MGTWR, and STWR, which incorporate spatial and temporal heterogeneity, effectively capture these dynamics. Wu et al. [73] emphasize the value of temporal dimensions in understanding socio-economic processes, while Han et al. [74] and Wang et al. [75] demonstrate the efficacy of these models in regions undergoing rapid transformation, such as China’s eastern Mega-region.

The modifiable areal unit problem (MAUP) further impacts the fitting outcomes of spatial–temporal models [76,77]. Parameters like HBN, GY, and PI, which correlate positively with GDP at the prefecture level, may exhibit negative correlations at the county level (Figures S1–S20). Openshaw [78] and Fotheringham and Wong [79] stress that MAUP-induced variability necessitates multi-scale regression approaches. Multi-scale analyses improve reliability by exploring the effects of spatial and temporal heterogeneity at varying scales [25,80]. Recent advancements, such as the One4All-ST framework [81], mitigate scale inconsistencies through flexible, unified spatio-temporal modeling.

Rational parameter selection also plays a crucial role. Indicators like HBN and PI offer insights into human development and infrastructure investment, while GY captures economic growth dynamics, making them essential for analyzing spatial–temporal

variations [75,82]. This aligns with Jiang and Yao [83], who underscore the importance of selecting indicators reflective of regional disparities in heterogeneous development landscapes like China. Therefore, adopting multi-scale models, flexible frameworks, and carefully selected parameters is crucial for addressing MAUP and enhancing the interpretability of spatial–temporal analyses. These approaches deepen our understanding of the interplay between spatial proximity, temporal dynamics, and socio-economic disparities while refining the application of Tobler’s First Law across varying scales.

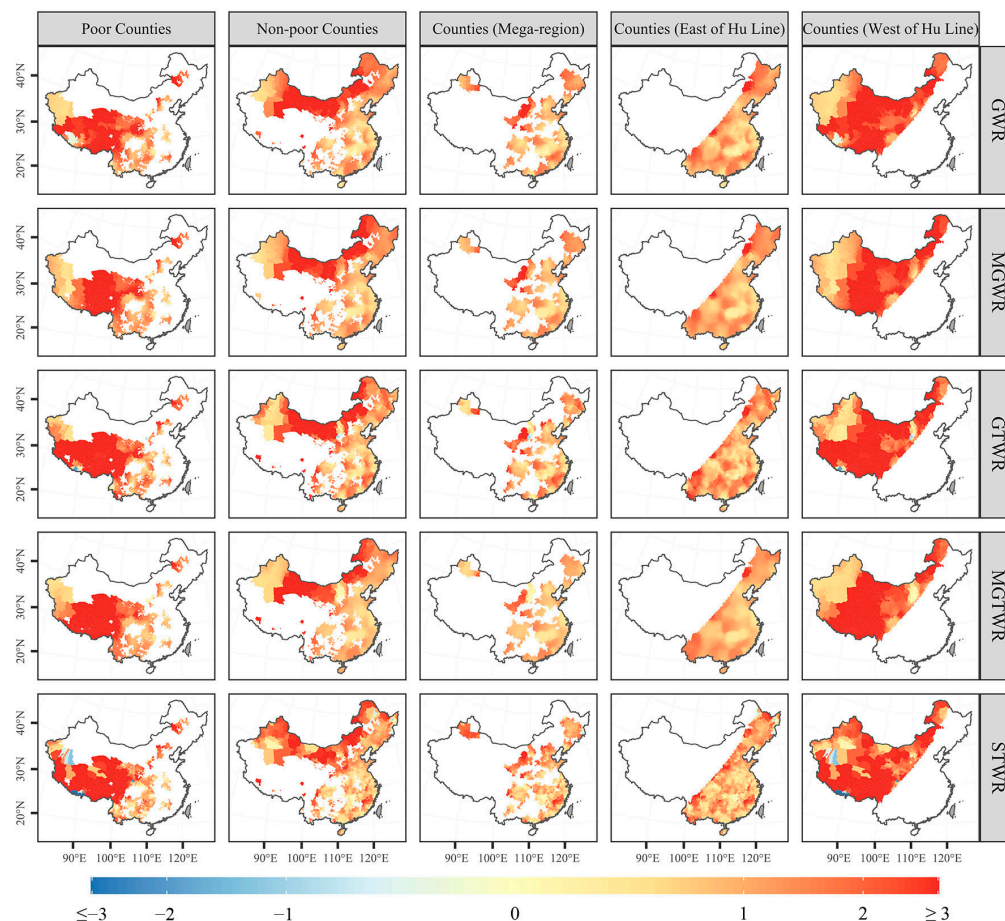


Figure 7. Spatio-temporal pattern of the β_k parameter for SI for different models across different regions at the county level in 2019.

5.4. Suggestions for Regional Disparity Alleviation

China has made great leaps in reducing poverty and reaching the benchmarks laid out in the Sustainable Development Goals (SDGs) [84,85], which has lifted more than 500 million of its citizens out of extreme poverty over the last three decades. Despite these achievements, regional disparities persist, necessitating a deeper understanding of the spatial and temporal dynamics of inequality to inform effective policy-making. This study, using the GWR, MGWR, GTWR, MGTWR and STWR models from 2000 to 2019, offers timely insights into the socio-economic variables influencing regional disparities across various scales (all counties, poverty-stricken and non-poverty-stricken counties, mega-regions, and sub-national levels). The results highlight several critical issues and policy implications.

Equalization of Public Services. One significant finding is the role of the public financial revenue (PFR) variable, which emerged as the second most important factor contributing to regional disparities from 2000 to 2020. This reflects the success of initiatives like the “China Rural Poverty Alleviation and Development (CRPAD) Program” [86,87]

in developing healthcare, education, and technology services in the central and western regions. However, other public service variables, such as SN and HBN, demonstrated weak relationships with economic growth, indicating potential misallocation of government resources. A similar point was also raised by Blanchard [88]. Therefore, this misallocation, characterized by overinvestment in manufacturing and underinvestment in domestic service industries, particularly at the county level, underscores the need for more balanced resource distribution. Insufficient equalization of public services remains a significant challenge for achieving high-quality economic development.

Rebalancing the Economy to Promote Domestic Consumption. When time interval variables were considered in the GTWR and STWR models, deposit balance (DB) emerged as a more significant factor than PFR in poverty-stricken regions and areas west of the Hu Line. This finding suggests that rising inter-regional inequality has contributed to high personal savings rates in these areas [89,90], highlighting the need to transition from high savings to higher domestic consumption [91]. Rebalancing the economy is essential for addressing these disparities, particularly in inland poverty-stricken regions and small cities, where fostering local demand could boost economic growth.

Monitoring County-Level Disparities and Addressing the MAUP Issue. The study confirmed Tobler's First Law of Geography, showing that adjacent counties tend to share more similar socio-economic determinants than distant ones. Patterns such as the positive congestive SI pattern in Xinjiang and the negative congestive DB pattern in the Pearl River Delta mega-regions highlight the importance of continuous monitoring and tailored interventions that account for the unique socio-economic and geographic characteristics of these regions. However, the analysis also revealed significant MAUP effects, particularly in regions with high inequities, such as Xinjiang and Inner Mongolia. For instance, the SI factor in Shaanxi varied in significance between county and mega-region scales, underscoring the need for cross-scale evaluations. Policies designed without considering scale variations may lead to inaccurate conclusions and ineffective interventions, making multi-scale analyses essential for designing robust and accurate policies to address regional disparities effectively [92,93].

Strategic Focus on High-Disparity Regions: Regions with pronounced inequities, such as Xinjiang and Inner Mongolia, require tailored strategies to address their unique challenges. These areas exhibit stronger MAUP effects and greater resource allocation needs, reinforcing the importance of targeted development efforts. Focusing on technical efficiency improvements and creating sustainable development models for these regions can significantly bridge the gap between high-growth and high-inequity areas, fostering equitable economic development [94–96].

5.5. Research Limitation

We should note that there is not one ideal dataset that can comprehensively represent the complexities of socially and economically meaningful regional inequity. Due to the data limitation of the China County Statistical Yearbook (CCSY) published by the National Bureau of Statistics of China, this study can only obtain 11 variables to delineate the regional variations. Meanwhile, to explore regional disparities, it is essential to address inflationary distortions in socio-economic data. In this study, the data collected from CCSY were adjusted using the same inflation coefficient, ensuring their robustness in demonstrating their contribution to nominal GDP per capita. However, if the goal is to analyze the variance of socio-economic data across different spatial and temporal scales, it would be advisable to account for inflation coefficients to achieve more accurate and comparable results. Moreover, different combinations of socio-economic indicators may lead to various alternative representations of regional disparity and different spatio-temporal patterns

in their relationships [90,93]. Therefore, it is crucial to integrate diverse socio-economic variables, such as remote sensing data, open access geographical data, etc., to study regional disparities and social perceptions of inequity in the future. The framework outlined in this study transforms static statistical data into multiple scales of geographical units but lacks ground truth data for validation. Therefore, it is advisable to employ composite indicators based on multiple dimensions of socio-economic and environmental features to further scrutinize the uncertainty and sensitivity of indicators in identifying inequities across different scales.

6. Conclusions

To better analyze the spatio-temporal dynamics of regional economic disparities in China, this study builds upon existing spatial and temporal regression models (e.g., GWR, MGWR, GTWR, and MGTWR) and advances the framework with the spatio-temporal weighted regression (STWR) model proposed by Que [34]. By introducing a “time distance” perspective, the study explores the intertwined spatial and temporal complexities of regional economic disparities. The contributions of this research can be summarized as follows:

- (1) **Extending Traditional Spatial Regression by Incorporating Temporal Dynamics.** Unlike models such as GWR, MGWR, GTWR, and MGTWR, which focus on spatially varying relationships at specific time steps, STWR incorporates a spatio-temporal kernel function. This kernel optimizes the weighting of observations based on their spatial and temporal proximity, enabling a more accurate representation of regional economic disparities where spatial and temporal non-stationarity coexist. This enhancement ensures a deeper understanding of the dynamic interactions driving disparities over time and space.
- (2) **Improving the Interpretability of Regional Disparities.** By employing county-level spatial units and analyzing disparities across diverse regions—poverty-stricken and non-poverty-stricken areas, mega-regions, and sub-national regions delineated by the Hu Line—STWR ensures robust estimation of regional disparities. The flexibility of spatial units enhances the model’s ability to reflect nuanced differences across various regions, making the results more interpretable and actionable for policymakers and stakeholders.
- (3) **Encouraging Data-Driven Policymaking.** This study successfully applies STWR to analyze a range of socio-economic variables, including primary and secondary industries, public financial revenue, and deposit balances, to assess regional economic disparities. By integrating spatial and temporal kernels, STWR provides a holistic analysis of socio-economic inequities, offering a comprehensive understanding of the factors driving disparities. This approach highlights specific spatial and temporal dimensions of inequality, enabling more targeted resource allocation and intervention strategies.

This study also emphasizes the practical applications of GTWR, MGTWR, and STWR models, which provide significant advancements in analyzing the spatial and temporal impacts of China’s “accurate poverty targeting” [97] initiatives and offer deeper insights into regional economic disparities. The key contributions are as follows:

- (1) **Impact of Industrialization on Regional Disparities.** Post-2000, heavy industry has intensified the rural–urban divide, particularly between mega- and non-mega-regions and areas west and east of the Hu Line. These findings highlight structural challenges in regional development, underscoring the need for tailored policies to address industrial dependency and promote balanced growth.
- (2) **Policy-Driven Transformations Post-2010.** The analysis of the public financial revenue (PFR) variable highlights the Chinese government’s focused efforts to improve public

services, ecological development, and capacity building, with a stronger impact observed in poverty-stricken areas. These results validate the effectiveness of targeted poverty alleviation strategies and provide a blueprint for scaling similar efforts.

- (3) Targeted Interventions to Address Disparities. Spatio-temporal insights identify specific counties where targeted investments in healthcare, education, and technology can effectively reduce inequities. The findings highlight the importance of sustained and region-specific policy efforts, particularly in poverty-stricken areas and regions west of the Hu Line. Enhancing technical efficiency and implementing long-term strategies can significantly contribute to equitable economic development and growth [89,90].

It is crucial to acknowledge that the effective application of GTWR, MGTWR, and STWR models hinges on the presence of spatio-temporal non-stationarity in parameters related to social disparities. Although socio-economic indicators may exhibit variations within spatial bandwidths and spatio-temporal kernels, relying solely on a combined measurement of spatial and temporal distances can lead to oversimplification or misinterpretation. Calculating distances in three dimensions—time and two-dimensional space—remains a significant methodological challenge. To address this, future research should focus on optimizing spatio-temporal kernel functions and experimenting with varying spatial and temporal bandwidths to more accurately capture the complexities of spatio-temporal heterogeneity.

Supplementary Materials: The following supporting information can be downloaded at: <https://www.mdpi.com/article/10.3390/land14010059/s1>.

Author Contributions: C.W.: conceptualization, writing. X.L. and W.C.: methodology, software application. L.Z.: data collection, data analysis. R.C. and W.W.: review, editing, manuscript revision. All authors contributed to the study. All authors have read and agreed to the published version of the manuscript.

Funding: This research was financially supported by the National Natural Science Foundation of China, NSFC Young Scientist Fund, No. 42201205; National Nature Science Foundation of China, NSFC General Fund, No. 42471443, and the Southern Marine Science and Engineering Guangdong Laboratory (Zhuhai) project No. 311021018.

Data Availability Statement: Data will be made available on request.

Conflicts of Interest: The authors have no competing interests to declare that are relevant to the content of this article.

References

- Pan, J.; Hu, Y. Spatial Identification of Multi-Dimensional Poverty in Rural China: A Perspective of Nighttime-Light Remote Sensing Data. *J. Indian Soc. Remote Sens.* **2018**, *46*, 1093–1111. [CrossRef]
- Kanbur, R.; Zhang, X. Fifty Years of Regional Inequality in China: A Journey Through Central Planning, Reform, and Openness. *Rev. Dev. Econ.* **2005**, *9*, 87–106. [CrossRef]
- Cingano, F. *Trends in Income Inequality and Its Impact on Economic Growth*; OECD: Paris, France, 2014.
- United Nations. The Inefficiency of Inequality. Available online: <https://www.un-ilibrary.org/content/books/9789210586283> (accessed on 7 June 2024).
- Wang, Y.; Chen, X.; Sun, P.; Liu, H.; He, J. Spatial-Temporal Evolution of the Urban-Rural Coordination Relationship in Northeast China in 1990–2018. *Chin. Geogr. Sci.* **2021**, *31*, 429–443. [CrossRef]
- Su, S.; Gong, Y.; Tan, B.; Pi, J.; Weng, M.; Cai, Z. Area Social Deprivation and Public Health: Analyzing the Spatial Non-Stationary Associations Using Geographically Weighed Regression. *Soc. Indic. Res.* **2017**, *133*, 819–832. [CrossRef]
- Zhang, G.; Chen, Y.; Wang, G.; Zhou, C. Spatial-Temporal Evolution and Influencing Factors of Digital Financial Inclusion: County-Level Evidence from China. *Chin. Geogr. Sci.* **2023**, *33*, 221–232. [CrossRef]
- Wei, C.; Cabrera Barona, P.; Blaschke, T. A New Look at Public Services Inequality: The Consistency of Neighborhood Context and Citizens' Perception across Multiple Scales. *ISPRS Int. J. Geo-Inf.* **2017**, *6*, 200. [CrossRef]

9. Wan, G. Accounting for Income Inequality in Rural China: A Regression-Based Approach. *J. Comp. Econ.* **2004**, *32*, 348–363. [[CrossRef](#)]
10. Anselin, L.; Getis, A. Spatial Statistical Analysis and Geographic Information Systems. *Ann. Reg. Sci.* **1992**, *26*, 19–33. [[CrossRef](#)]
11. Cabrera-Barona, P.; Wei, C.; Hagenlocher, M. Multiscale Evaluation of an Urban Deprivation Index: Implications for Quality of Life and Healthcare Accessibility Planning. *Appl. Geogr.* **2016**, *70*, 1–10. [[CrossRef](#)]
12. Casetti, E. Bayesian Regression and the Expansion Method. *Geogr. Anal.* **1992**, *24*, 58–74. [[CrossRef](#)]
13. Gutiérrez, J.; Cardozo, O.D.; García-Palomares, J.C. Transit Ridership Forecasting at Station Level: An Approach Based on Distance-Decay Weighted Regression. *J. Transp. Geogr.* **2011**, *19*, 1081–1092. [[CrossRef](#)]
14. Brunson, C.; Fotheringham, A.S.; Charlton, M.E. Geographically Weighted Regression: A Method for Exploring Spatial Nonstationarity. *Geogr. Anal.* **1996**, *28*, 281–298. [[CrossRef](#)]
15. Xu, Z.; Cai, Z.; Wu, S.; Huang, X.; Liu, J.; Sun, J.; Su, S.; Weng, M. Identifying the Geographic Indicators of Poverty Using Geographically Weighted Regression: A Case Study from Qiandongnan Miao and Dong Autonomous Prefecture, Guizhou, China. *Soc. Indic. Res.* **2019**, *142*, 947–970. [[CrossRef](#)]
16. Shen, X.; Zhou, Y.; Jin, S.; Wang, D. Spatiotemporal Influence of Land Use and Household Properties on Automobile Travel Demand. *Transp. Res. Part D Transp. Environ.* **2020**, *84*, 102359. [[CrossRef](#)]
17. Wei, Y.D. Spatiality of Regional Inequality. *Appl. Geogr.* **2015**, *61*, 1–10. [[CrossRef](#)]
18. Yuan, X.; Li, Y.; Song, Y.; Lu, H.; Wang, Y.; Ge, B.; Wang, J. Spatial Distribution Characteristics and Driving Factors of 777 Traditional Villages in Yunnan Province: A Study Based on GWR Model and Geodetector. *Land* **2024**, *13*, 2004. [[CrossRef](#)]
19. Zhang, X.; Du, L.; Song, X. Identification of Urban Renewal Potential Areas and Analysis of Influential Factors from the Perspective of Vitality Enhancement: A Case Study of Harbin City's Core Area. *Land* **2024**, *13*, 1934. [[CrossRef](#)]
20. Shi, T.; Xu, H.; Bai, X. Spatiotemporal Evaluation and Driving Factor Screening for Regulating and Supporting Ecosystem Service Values in Suzhou–Wuxi–Changzhou Metropolitan Area's Green Space. *Land* **2024**, *13*, 1191. [[CrossRef](#)]
21. Li, B.; Lu, Y.; Li, Y.; Zuo, H.; Ding, Z. Research on the Spatiotemporal Distribution Characteristics and Accessibility of Traditional Villages Based on Geographic Information Systems—A Case Study of Shandong Province, China. *Land* **2024**, *13*, 1049. [[CrossRef](#)]
22. Lu, B.; Brunson, C.; Charlton, M.; Harris, P. Geographically Weighted Regression with Parameter-Specific Distance Metrics. *Int. J. Geogr. Inf. Sci.* **2017**, *31*, 982–998. [[CrossRef](#)]
23. Wei, C.; Cabrera-Barona, P.; Blaschke, T. Local Geographic Variation of Public Services Inequality: Does the Neighborhood Scale Matter? *Int. J. Environ. Res. Public Health* **2016**, *13*, 981. [[CrossRef](#)] [[PubMed](#)]
24. Fotheringham, A.S.; Yang, W.; Kang, W. Multiscale Geographically Weighted Regression (MGWR). *Ann. Am. Assoc. Geogr.* **2017**, *107*, 1247–1265. [[CrossRef](#)]
25. Wu, C.; Ren, F.; Hu, W.; Du, Q. Multiscale Geographically and Temporally Weighted Regression: Exploring the Spatiotemporal Determinants of Housing Prices. *Int. J. Geogr. Inf. Sci.* **2019**, *33*, 489–511. [[CrossRef](#)]
26. Tong, Z.; Kong, Z.; Jia, X.; Zhang, H.; Zhang, Y. Multiscale Impact of Environmental and Socio-Economic Factors on Low Physical Fitness among Chinese Adolescents and Regionalized Coping Strategies. *Int. J. Environ. Res. Public Health* **2022**, *19*, 13504. [[CrossRef](#)] [[PubMed](#)]
27. Soranno, P.A.; Cheruvilil, K.S.; Bissell, E.G.; Bremigan, M.T.; Downing, J.A.; Fergus, C.E.; Filstrup, C.T.; Henry, E.N.; Lottig, N.R.; Stanley, E.H.; et al. Cross-Scale Interactions: Quantifying Multi-Scaled Cause–Effect Relationships in Macrosystems. *Front. Ecol. Environ.* **2014**, *12*, 65–73. [[CrossRef](#)]
28. Rollinson, C.R.; Finley, A.O.; Alexander, M.R.; Banerjee, S.; Dixon Hamil, K.-A.; Koenig, L.E.; Locke, D.H.; DeMarche, M.L.; Tingley, M.W.; Wheeler, K.; et al. Working across Space and Time: Nonstationarity in Ecological Research and Application. *Front. Ecol. Environ.* **2021**, *19*, 66–72. [[CrossRef](#)]
29. Huang, B.; Wu, B.; Barry, M. Geographically and Temporally Weighted Regression for Modeling Spatio-Temporal Variation in House Prices. *Int. J. Geogr. Inf. Sci.* **2010**, *24*, 383–401. [[CrossRef](#)]
30. Wei, Q.; Zhang, L.; Duan, W.; Zhen, Z. Global and Geographically and Temporally Weighted Regression Models for Modeling PM2.5 in Heilongjiang, China from 2015 to 2018. *Int. J. Environ. Res. Public Health* **2019**, *16*, 5107. [[CrossRef](#)] [[PubMed](#)]
31. Hu, J.; Zhang, J.; Li, Y. Exploring the Spatial and Temporal Driving Mechanisms of Landscape Patterns on Habitat Quality in a City Undergoing Rapid Urbanization Based on GTWR and MGWR: The Case of Nanjing, China. *Ecol. Indic.* **2022**, *143*, 109333. [[CrossRef](#)]
32. Zhang, J.; Dong, Z. Assessment of Coupling Coordination Degree and Water Resources Carrying Capacity of Hebei Province (China) Based on WRESP2D2P Framework and GTWR Approach. *Sustain. Cities Soc.* **2022**, *82*, 103862. [[CrossRef](#)]
33. Fotheringham, A.S.; Crespo, R.; Yao, J. Geographical and Temporal Weighted Regression (GTWR). *Geogr. Anal.* **2015**, *47*, 431–452. [[CrossRef](#)]
34. Que, X.; Ma, C.; Ma, X.; Chen, Q. Parallel Computing for Fast Spatiotemporal Weighted Regression. *Comput. Geosci.* **2021**, *150*, 104723. [[CrossRef](#)]

35. Wu, Y.; Kan, H.; Deng, A. Spatio-Temporal Correlation and Optimization of Urban Development Characteristics and Carbon Balance in Counties: A Case Study of the Anhui Province, China. *Land* **2024**, *13*, 810. [[CrossRef](#)]
36. Yang, L.; Xu, Y.; Zhu, J.; Sun, K. Spatiotemporal Evolution and Influencing Factors of the Coupling Coordination of Urban Ecological Resilience and New Quality Productivity at the Provincial Scale in China. *Land* **2024**, *13*, 1998. [[CrossRef](#)]
37. Wang, X.; Liu, Y. Enhancing Agricultural Ecological Efficiency in China: An Evolution and Pathways under the Carbon Neutrality Vision. *Land* **2024**, *13*, 187. [[CrossRef](#)]
38. Que, X.; Ma, X.; Ma, C.; Chen, Q. A Spatiotemporal Weighted Regression Model (STWR v1.0) for Analyzing Local Nonstationarity in Space and Time. *Geosci. Model Dev.* **2020**, *13*, 6149–6164. [[CrossRef](#)]
39. Mansour, S.; Al Kindi, A.; Al-Said, A.; Al-Said, A.; Atkinson, P. Sociodemographic Determinants of COVID-19 Incidence Rates in Oman: Geospatial Modelling Using Multiscale Geographically Weighted Regression (MGWR). *Sustain. Cities Soc.* **2021**, *65*, 102627. [[CrossRef](#)] [[PubMed](#)]
40. Johnston, R.J. Local Effects in Voting at a Local Election. *Ann. Assoc. Am. Geogr.* **1974**, *64*, 418–429. [[CrossRef](#)]
41. Hanson, H.A.; Martin, C.; O'Neil, B.; Leiser, C.L.; Mayer, E.N.; Smith, K.R.; Lowrance, W.T. The Relative Importance of Race Compared to Health Care and Social Factors in Predicting Prostate Cancer Mortality: A Random Forest Approach. *J. Urol.* **2019**, *202*, 1209–1216. [[CrossRef](#)]
42. Luo, Y.; Su, S. SpatioTemporal Random Forest and SpatioTemporal Stacking Tree: A Novel Spatially Explicit Ensemble Learning Approach to Modeling Non-Linearity in Spatiotemporal Non-Stationarity. *Int. J. Appl. Earth Obs. Geoinf.* **2025**, *136*, 104315. [[CrossRef](#)]
43. Bindajam, A.A.; Mallick, J.; Talukdar, S.; Shahfahad; Shohan, A.A.A.; Rahman, A. Modeling the Spatiotemporal Heterogeneity of Land Surface Temperature and Its Relationship with Land Use Land Cover Using Geo-Statistical Techniques and Machine Learning Algorithms. *Environ. Sci. Pollut. Res.* **2023**, *30*, 106917–106935. [[CrossRef](#)] [[PubMed](#)]
44. Georganos, S.; Grippa, T.; Niang Gadiaga, A.; Linard, C.; Lennert, M.; Vanhuyse, S.; Mboga, N.; Wolff, E.; Kalogirou, S. Geographical Random Forests: A Spatial Extension of the Random Forest Algorithm to Address Spatial Heterogeneity in Remote Sensing and Population Modelling. *Geocarto Int.* **2021**, *36*, 121–136. [[CrossRef](#)]
45. Liu, R.; Yuan, H.; Chen, W.; Hu, Q.; Zhou, M.; Bao, L. Spatio-Temporal Heterogeneity and Scenario Prediction of Influencing Factors of Transportation Carbon Emissions in the Yangtze River Economic Belt, China. *Environ. Res. Commun.* **2024**, *6*, 115022. [[CrossRef](#)]
46. Tang, B.; Ma, K.; Liu, Y.; Wang, X.; Tang, S.; Xiao, Y.; Cheke, R.A. Managing Spatio-Temporal Heterogeneity of Susceptibles by Embedding It into an Homogeneous Model: A Mechanistic and Deep Learning Study. *PLoS Comput. Biol.* **2024**, *20*, e1012497. [[CrossRef](#)]
47. Chen, R.; Wang, C.; Que, X.; Liao, F.H.; Ma, X.; Wang, Z.; Li, Z.; Wen, K.; Lai, Y.; Xu, X. Exploring Urban Heat Distribution and Thermal Comfort Exposure Using Spatiotemporal Weighted Regression (STWR). *Buildings* **2024**, *14*, 1883. [[CrossRef](#)]
48. Wang, Z.; Que, X.; Li, M.; Liu, Z.; Shi, X.; Ma, X.; Fan, C.; Lin, Y. Spatiotemporally Weighted Regression (STWR) for Assessing Lyme Disease and Landscape Fragmentation Dynamics in Connecticut Towns. *Ecol. Inform.* **2024**, *84*, 102870. [[CrossRef](#)]
49. Yang, Z.; Zhang, X.; Lei, J.; Duan, Z.; Li, J. Spatio-Temporal Pattern Characteristics of Relationship Between Urbanization and Economic Development at County Level in China. *Chin. Geogr. Sci.* **2019**, *29*, 553–567. [[CrossRef](#)]
50. Jianghui, W.J. Types, Characteristics and Tendency of County-Level Administrative Division Adjustment in China since 2000. *Trop. Geogr.* **2018**, *38*, 799–809. [[CrossRef](#)]
51. Todaro, M.P.; Smith, S.C. *Economic Development*, 13th ed.; Pearson: Hoboken, NJ, USA, 2020; ISBN 978-1-292-29115-4.
52. Lewis, W.A. Economic Development with Unlimited Supplies of Labour. *Manch. Sch.* **1954**, *22*, 139–191. [[CrossRef](#)]
53. Baneliené, R. Industry Impact on GDP Growth in Developed Countries under R&D Investment Conditions. *J. Small Bus. Strategy (Arch. Only)* **2021**, *31*, 66–80.
54. Zhang, J. Data Analysis of Fiscal Expenditure and GDP Based on Financial Budget Performance Evaluation Indicators. *Discret. Dyn. Nat. Soc.* **2022**, *2022*, 1141618. [[CrossRef](#)]
55. Barro, R.J. Government Spending in a Simple Model of Endogenous Growth. *J. Political Econ.* **1990**, *98*, S103–S125. [[CrossRef](#)]
56. Bai, Y. An Empirical Analysis of the Relationship Between Chinese GDP and Deposit Savings. In Proceedings of the 7th International Conference on Economic Management and Green Development, Oxford, UK, 6 August 2023; Li, X., Yuan, C., Kent, J., Eds.; Springer Nature: Singapore, 2024; pp. 873–884.
57. Rachuba, J. GDP Growth as a Bank Loan Quality Determinant. *J. Bank. Financ. Econ.* **2020**, *14*, 21–37. [[CrossRef](#)]
58. Chen, X.; Shuai, C.; Zhang, Y.; Wu, Y. Decomposition of Energy Consumption and Its Decoupling with Economic Growth in the Global Agricultural Industry. *Environ. Impact Assess. Rev.* **2020**, *81*, 106364. [[CrossRef](#)]
59. Bloom, D.; Canning, D. Health as Human Capital and Its Impact on Economic Performance. *Geneva Pap. Risk Insur. Issues Pract.* **2003**, *28*, 304–315. [[CrossRef](#)]
60. Strydom, N.; Struweg, J. Malthus Revisited: Long-Term Trends in South African Population Growth and Agricultural Output. *Agrekon* **2016**, *55*, 34–61. [[CrossRef](#)]

61. Wu, B.; Li, R.; Huang, B. A Geographically and Temporally Weighted Autoregressive Model with Application to Housing Prices. *Int. J. Geogr. Inf. Sci.* **2014**, *28*, 1186–1204. [[CrossRef](#)]
62. Lu, B.; Harris, P.; Charlton, M.; Brunsdon, C. The GWmodel R Package: Further Topics for Exploring Spatial Heterogeneity Using Geographically Weighted Models. *Geo-Spat. Inf. Sci.* **2014**, *17*, 85–101. [[CrossRef](#)]
63. Hong, Z.; Mei, C.; Wang, H.; Du, W. Spatiotemporal Effects of Climate Factors on Childhood Hand, Foot, and Mouth Disease: A Case Study Using Mixed Geographically and Temporally Weighted Regression Models. *Int. J. Geogr. Inf. Sci.* **2021**, *35*, 1611–1633. [[CrossRef](#)]
64. Hong, Z.; Wang, J.; Wang, H. Introducing Bootstrap Test Technique to Identify Spatial Heterogeneity in Geographically and Temporally Weighted Regression Models. *Spat. Stat.* **2022**, *51*, 100683. [[CrossRef](#)]
65. Li, Z.; Fotheringham, A.S. Computational Improvements to Multi-Scale Geographically Weighted Regression. *Int. J. Geogr. Inf. Sci.* **2020**, *34*, 1378–1397. [[CrossRef](#)]
66. Tobler, W.R. A Computer Movie Simulating Urban Growth in the Detroit Region. *Econ. Geogr.* **1970**, *46*, 234–240. [[CrossRef](#)]
67. Zhang, W. Rethinking Regional Disparity in China. *Econ. Plan.* **2001**, *34*, 113–138. [[CrossRef](#)]
68. Li, Z.; He, S.; Su, S.; Li, G.; Chen, F. Public Services Equalization in Urbanizing China: Indicators, Spatiotemporal Dynamics and Implications on Regional Economic Disparities. *Soc. Indic. Res.* **2020**, *152*, 1–65. [[CrossRef](#)]
69. Song, L.; Wang, P.; Xiang, K.; Chen, W.-Q. Regional Disparities in Decoupling Economic Growth and Steel Stocks: Forty Years of Provincial Evidence in China. *J. Environ. Manag.* **2020**, *271*, 111035. [[CrossRef](#)]
70. Chen, A. Reducing China's Regional Disparities: Is There a Growth Cost? *China Econ. Rev.* **2010**, *21*, 2–13. [[CrossRef](#)]
71. Kanbur, R.; Wan, G.; Zhang, X. Introduction: Growing Inequality in China. *J. Asia Pac. Econ.* **2005**, *10*, 405–407. [[CrossRef](#)]
72. Gao, J.; Liu, Y.; Chen, J.; Cai, Y. Demystifying the Geography of Income Inequality in Rural China: A Transitional Framework. *J. Rural Stud.* **2022**, *93*, 398–407. [[CrossRef](#)]
73. Wu, S.; Wang, Z.; Du, Z.; Huang, B.; Zhang, F.; Liu, R. Geographically and Temporally Neural Network Weighted Regression for Modeling Spatiotemporal Non-Stationary Relationships. *Int. J. Geogr. Inf. Sci.* **2021**, *35*, 582–608. [[CrossRef](#)]
74. Han, L.; Zhang, X.; Zhou, W.; Shen, M.; Huang, Y.; Li, W.; Qian, Y. Transformation of China's Urbanization and Eco-Environment Dynamics: An Insight with Location-Based Population-Weighted Indicators. *Environ. Sci. Pollut. Res.* **2021**, *28*, 16558–16567. [[CrossRef](#)] [[PubMed](#)]
75. Wang, H.; Zhang, B.; Liu, Y.; Liu, Y.; Xu, S.; Zhao, Y.; Chen, Y.; Hong, S. Urban Expansion Patterns and Their Driving Forces Based on the Center of Gravity-GTWR Model: A Case Study of the Beijing-Tianjin-Hebei Urban Agglomeration. *J. Geogr. Sci.* **2020**, *30*, 297–318. [[CrossRef](#)]
76. Iyanda, A.E.; Osayomi, T. Is There a Relationship between Economic Indicators and Road Fatalities in Texas? A Multiscale Geographically Weighted Regression Analysis. *GeoJournal* **2021**, *86*, 2787–2807. [[CrossRef](#)]
77. Fotheringham, A.S.; Sachdeva, M. Scale and Local Modeling: New Perspectives on the Modifiable Areal Unit Problem and Simpson's Paradox. *J. Geogr. Syst.* **2022**, *24*, 475–499. [[CrossRef](#)]
78. Openshaw, S. Ecological Fallacies and the Analysis of Areal Census Data. *Environ. Plan A* **1984**, *16*, 17–31. [[CrossRef](#)] [[PubMed](#)]
79. Fotheringham, A.S.; Wong, D.W.S. The Modifiable Areal Unit Problem in Multivariate Statistical Analysis. *Environ. Plan A* **1991**, *23*, 1025–1044. [[CrossRef](#)]
80. Yan, J.; Wu, B.; Zheng, H. Multiscale Cooperative Optimization in Multiscale Geographically Weighted Regression Models. *Int. J. Geogr. Inf. Sci.* **2024**, *1*–20. [[CrossRef](#)]
81. Chen, L.; Fang, J.; Liu, T.; Cao, S.; Wang, L. A Unified Model for Spatio-Temporal Prediction Queries with Arbitrary Modifiable Areal Units. In Proceedings of the 2024 IEEE 40th International Conference on Data Engineering (ICDE), Utrecht, The Netherlands, 13–16 May 2024; pp. 1352–1365.
82. Jiang, Y.; Shi, C. Estimating Sustainability and Regional Inequalities Using an Enhanced Sustainable Development Index in China. *Sustain. Cities Soc.* **2023**, *99*, 104555. [[CrossRef](#)]
83. Jiang, Y. Trade Integration and Regional Inequality: A Theoretical Framework with Empirical Implications for China. *J. Chin. Econ. Bus. Stud.* **2016**, *14*, 365–384. [[CrossRef](#)]
84. Liu, X.; Yuan, M. Assessing Progress towards Achieving the Transport Dimension of the SDGs in China. *Sci. Total Environ.* **2023**, *858*, 159752. [[CrossRef](#)] [[PubMed](#)]
85. Cao, M.; Chen, M.; Zhang, J.; Pradhan, P.; Guo, H.; Fu, B.; Li, Y.; Bai, Y.; Chang, L.; Chen, Y.; et al. Spatio-Temporal Changes in the Causal Interactions among Sustainable Development Goals in China. *Humanit. Soc. Sci. Commun.* **2023**, *10*, 450. [[CrossRef](#)]
86. Zhou, Y.; Liu, Z.; Wang, H.; Cheng, G. Targeted Poverty Alleviation Narrowed China's Urban-Rural Income Gap: A Theoretical and Empirical Analysis. *Appl. Geogr.* **2023**, *157*, 103000. [[CrossRef](#)]
87. Ge, Y.; Hu, S.; Song, Y.; Zheng, H.; Liu, Y.; Ye, X.; Ma, T.; Liu, M.; Zhou, C. Sustainable Poverty Reduction Models for the Coordinated Development of the Social Economy and Environment in China. *Sci. Bull.* **2023**, *68*, 2236–2246. [[CrossRef](#)]
88. Blanchard, O.; Bean, C.; Münchau, W. European Unemployment: The Evolution of Facts and Ideas. *Econ. Policy* **2006**, *21*, 7–59. [[CrossRef](#)]

89. Fleisher, B.; Li, H.; Zhao, M.Q. Human Capital, Economic Growth, and Regional Inequality in China. *J. Dev. Econ.* **2010**, *92*, 215–231. [[CrossRef](#)]
90. van Treeck, T.; Sturn, S. *Income Inequality as a Cause of the Great Recession? A Survey of Current Debates*; International Labour Organization: Geneva, Switzerland, 2012.
91. Lewin, P.A.; Watson, P.; Brown, A. Surviving the Great Recession: The Influence of Income Inequality in US Urban Counties. *Reg. Stud.* **2018**, *52*, 781–792. [[CrossRef](#)]
92. Ezcurra, R.; Pascual, P.; Rapún, M. The Dynamics of Regional Disparities in Central and Eastern Europe during Transition. *Eur. Plan. Stud.* **2007**, *15*, 1397–1421. [[CrossRef](#)]
93. Voskamp, I.M.; Visscher, M.N.; Vreugdenhil, C.; Van Lammeren, R.J.A.; Sutton, N.B. Spatial, Infrastructural and Consumer Characteristics Underlying Spatial Variability in Residential Energy and Water Consumption in Amsterdam. *Sustain. Cities Soc.* **2021**, *72*, 102977. [[CrossRef](#)]
94. Feldman, M.P.; Florida, R. The Geographic Sources of Innovation: Technological Infrastructure and Product Innovation in the United States. *Ann. Assoc. Am. Geogr.* **1994**, *84*, 210–229. [[CrossRef](#)]
95. Doloreux, D. What We Should Know about Regional Systems of Innovation. *Technol. Soc.* **2002**, *24*, 243–263. [[CrossRef](#)]
96. Zhao, X.; Qian, Y. Does Digital Technology Promote Green Innovation Performance? *J. Knowl. Econ.* **2024**, *15*, 7568–7587. [[CrossRef](#)]
97. Tan, X.; Wang, Z.; An, Y.; Wang, W. Types and Optimization Paths Between Poverty Alleviation Effectiveness and Rural Revitalization: A Case Study of Hunan Province, China. *Chin. Geogr. Sci.* **2023**, *33*, 966–982. [[CrossRef](#)]

Disclaimer/Publisher’s Note: The statements, opinions and data contained in all publications are solely those of the individual author(s) and contributor(s) and not of MDPI and/or the editor(s). MDPI and/or the editor(s) disclaim responsibility for any injury to people or property resulting from any ideas, methods, instructions or products referred to in the content.